A Poincaré Image-Based Detector of ECG Segments Containing Atrial and Ventricular Beats

Guadalupe García-Isla[1], Luca Mainardi[1], Valentina DA Corino[1]

[1] Department of Electronics, Information and Bioengineering (DEIB), Politecnico di Milano, Milano, Italy

Abstract

An electrocardiogram (ECG) classifier for the detection of ECG segments containing atrial or ventricular (A/V) beats could ease in the detection of premature atrial complexes (PACs) and by so, the study of their relationship with atrial fibrillation (AF) and stroke. In this work such a classifier is presented based on convolutional neural networks (CNN) and the RR and dRR interval representation on Poincaré Images. Two PhysioNet open-source databases containing beat annotations were used. ECG signals were divided into 30-beat segments with a 50% overlap. Each segment was then transformed into a Poincaré Image. A total of 381151 and 62142 Poincaré Images were computed for normal (N) and A/V segments. RR, dRR and both types of Poincaré Images combined were evaluated as inputs to the CNN. The CNN was trained following a patient-wise train-test division (i.e., no patient was included both in the train and test set) in a 10-fold cross-validation. The patient-wise median and interquartile range accuracy, sensitivity and positive predictive values were 97.90 (94.49 - 99.28), 96.03 (89.67 - 98.76) and 91.91 (70.87 - 99.24), respectively for RR input. No statistical significant differences in performance were found among the three types of Poincaré Images input. Results suggest the present methodology manages to distinguish among N and A/V with high precision.

1. Introduction

Premature atrial complexes (PACs) and premature ventricular complexes (PVCs) account for beats originating in a site different than the sinoatrial node; the atrium and the ventricles, respectively. PACs are generally considered benign and without any relevant clinical implications. However, late studies link frequent PACs with the first time appearance of atrial fibrillation (AF), myocardium deterioration and increased risk for stroke [1–3].

Despite the evidence of the possible implications of PACs, no clear relationship between PACs and the enumerated events has been described. Even if frequent PACs have been related to paroxysmal AF (PAF) [1] no proper definition of frequent PAC has been formulated. Moreover, PAC relationship with stroke is still controversial [2, 3]. The further elucidation of the direct and indirect implications of PACs would require of the analysis of long-term electrocardiogram (ECG) recordings and automatic PAC detectors could ease the study of this phenomenon.

Numerous beat classifiers are present in literature [4, 5], few developed specifically for PAC detection and none of them attaining a sensitivity and positive predictive value (PPV) high enough so as to be reliable for drawing meaningful conclusions about their implications [4]. Both ventricular (including PVCs) and atrial (including PACs) alter RR intervals (the distance between subsequent R peaks) similarly. However, while ventricular beats induce large QRS complex amplitude distortions, atrial beats cause low amplitude P-wave alterations. The presence of noise, ECG morphological inter-patient variability and P-wave parametrization complexity makes PAC detection a challenging matter. While R peak detection and RR intervals are robust against noise and easily quantifiable, P-wave morphology study entails a higher complexity. A detector based on RR intervals to detect ECG segments containing any type of atrial or ventricular beat (from now on referred as A/V) could reduce the ECG segments to be analyzed. In addition, if coupled with and already existing automatic beat classifier, it would reduce false positives and ease the identification of false negatives.

This work presents an automatic A/V ECG segment classifier based on the Poincaré Image representation of RR intervals as described in [6] and convolutional neural networks (CNN). The presented classifier enables the detection of regions containing A/V beats, drastically reducing the workload for manual beat annotations. This could ease the study of the PAC implications, currently hampered by the unavailability of extensive annotated databases and the high number of hours required to perform such task by specialized clinicians. Furthermore, the present methodology could be used as a complementary detector to the beat-

to-beat classifiers present in literature, what could lead to more reliant automatic annotations.

2. Materials and Methods

2.1. Data

Two open source PhysioNet databases were used in this study, the Supraventricular Arrhythmia Database (SVDB) and the Long-term ST Database (LTSTDB) [7]. The SVDB contains 78 ECG recordings of 30 minutes duration and 250 Hz sampling frequency. The LTSTDB instead, contains 86 ECG traces from 80 patients of 21 to 24 hours duration sampled at 128 Hz. Both databases contain 2-lead ECGs with manual beat-to-beat annotations. From the public databases available with manual beat annotations these are those containing a higher amount of PACs. While the LTSTDB contains a high number of isolated and frequent PACs in the presence of different ST alterations, the SVDB offers a complete gathering of the different supraventricular beat patters. Table 1 displays the beat annotations present in the databases and which of them were considered as A/V.

2.2. Poincaré Images

ECG signals were divided into 30-beat segments with 50% overlap using the QRS annotations provided in each database. From each segment, the RR and the dRR sequences were computed. While the RR sequence is defined as distance between subsequent R peaks i.e. $RR_i = R_i - R_{i-1}$, the dRR stands for the difference of subsequent RR intervals i.e. $dRR_i = RR_i - RR_{i-1}$.

The Poincaré Plot is a graphic representation of one RR_i (or dRR_i) plotted against the previous one, RR_{i-1} (or dRR_{i-1}). Poincaré Images were computed by binarizing the space of the Poincaré Plot for both RR and dRR as in [6]. Following the study in [6] the bin size was set to 40 ms and the Poincaré Images ranges were set to [0, 1600] ms and [-800, 800] ms in both x and y-axis for RR and dRR images, respectively. Poincaré Images containing at least one beat labelled as A/V were labelled as A/V whereas those not containing any beat of the mentioned categories were labelled as N.

2.3. Classification model

A CNN was used for classification of the described Poincaré Images. Three different types of inputs were tested: RR, dRR and both. In all cases the model was a 2D CNN with 25 layers, kernel size of (3, 3), (1, 1) stride and ReLu activation function, followed by a max pooling layer, a fully connected layer with 100 hidden units and a final sigmoid activation layer. The model was trained using the Adam optimizer and binary cross-entropy as loss function.

2.4. Statistical analysis

For analysing the performance of the proposed methodology a 10-Fold cross-validation with patient-wise (i.e. no patient was both included in both the training and test set) train-test division was performed. A Kruskal–Wallis one-way analysis of variance test with Bonferroni Post-Host correction was performed to study the best input option for representing the differences between N and A/V from a patient-wise performance perspective.

3. Results

3.1. Poincaré Images

Table 2 gathers the total amount of Poincaré Images computed for each database and type of image. In Figure 1 an example of N and A/V Poincaré Images is shown for an RR Poincaré Plot (first column), an RR and a dRR Poincaré Image. N Poincaré Plot and Images condensed all samples in a single cluster as R peaks distance follow a regular behaviour. In contrast, as A/V beats disrupt the RR sequence, A/V images contained outlier points independent of the main cluster.

3.2. Performance

The classifier performance was evaluated from two different perspectives: element-wise i.e., each Poincaré Image was treated as an individual sample regardless of the patient it belonged to (Table 3) and patient-wise i.e., performance was calculated for each specific patient (Table 4). Analysis of classification not taking into account patient dependencies as in Table 3 disregards the fact that not all patients accounted for the same number of A/V images, and thus offers a biased view of the overall classifier performance. Results from patient-wise perspective in Table 4 are expressed as the median performance per patient together with the 75 and 25-percentile. No statistical significant differences between RR, dRR and $RR + dRR$ inputs were appreciated. On Figure 2 the patient-specific accuracy, sensitivity, specificity and positive predictive value (PPV) distribution is displayed. As it can be seen, although most patients exhibited high performance results, outliers were present in all metrics.

4. Discussion

In this study a novel method for the detection of ECG segments containing atrial or ventricular beats is presented. The methodology relies on a 2D representation of RR in-

Table 1. PhysioNet and simplified beat annotations per database.

Labelling	N				A/V							
Beat Annotations	B	N	e	Q	A	a	S	V	F	E	J	j
LTSTDB	88720	6727000	22	2	5482	29	30820	39840	476	71	1	6
SVDB	1	162100	0	80	0	1	12090	9930	23	0	9	0

B stands for bundle branche block beat, N for normal beat, A for atrial premature beat, a for aberrated atrial premature beat, e for atrial escape beat, Q for unclassifiable beat, S for supraventricular premature or ectopic beat (atrial or nodal), V for premature ventricular contraction, F fusion of ventricular and normal beat, E for ventricular escape beat, J for nodal (junctional) premature beat and j for nodal (junctional) escape beat.

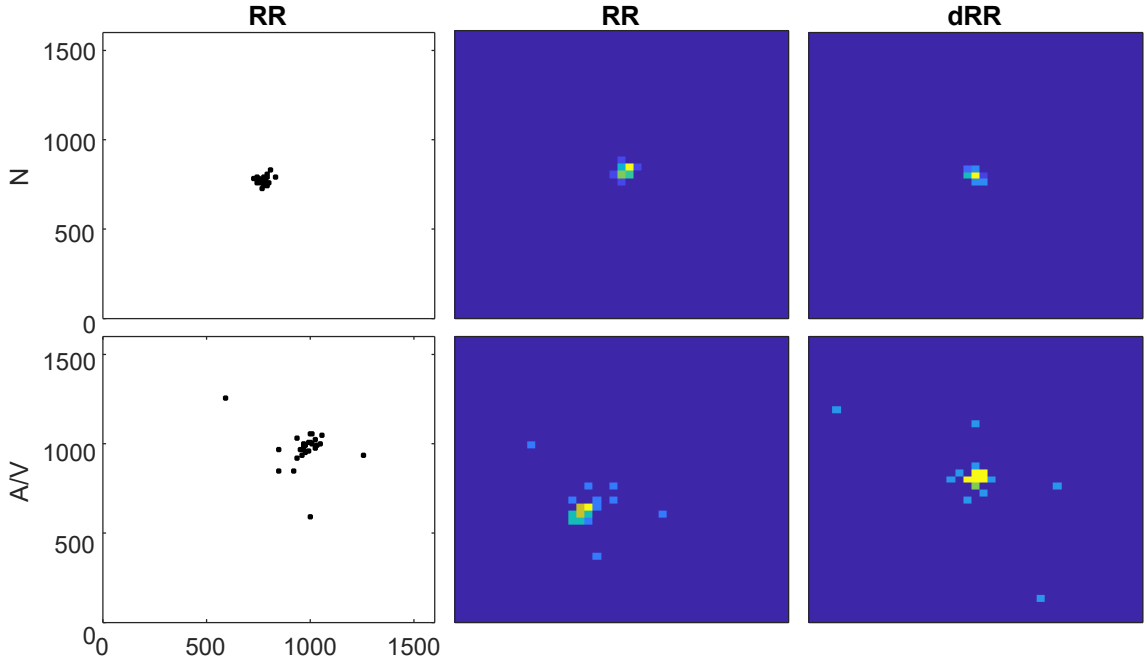

Figure 1. Poincaré Plot (first column) and Poincaré Image (second and third column) examples for RR (second column) and dRR (third column) configurations for 30-beat ECG segments for N (first row) and A/V (second row).

Table 2. Poincaré Images computed for each category per database.

Database (DB)	#Patients	N	A/V
SVDB	78	377156	53847
LTSTDB	80	3995	8295
Total	158	381151	62142

Table 3. Classification performance on the total of Poincaré Images classified in all K-folds.

	RR	dRR	RR + dRR
Accuracy (%)	95.94	96.16	96.05
Sensitivity (%)	92.00	94.88	93.84
Specificity (%)	96.59	96.36	96.41
PPV (%)	81.46	80.96	80.99

tervals to capture their non-linear dynamics. The fact that it solely relies on R peak detection, makes this methodology more robust against noise presence than those based on morphological waveform analysis. Performance was analyzed from both a patient-wise and an element-wise point of view (Table 3 and 4, respectively). Three different Poincaré Image inputs were studied without appreciation of significant differences in patient-wise performance. In all cases, accuracy was superior to 96%, sensitivity higher than 93% and PPV superior to 80%. Given the unbalance nature of the dataset, as shown in Table 2, the decrease in PPV accounted for false positives in a greater proportion than false negatives (as sensitivity values were kept high).

Table 4. Patient-wise classification performance. Values are expressed as median (75-percentile, 25-percentile).

	RR	dRR	RR + dRR
Accuracy (%)	97.90 (94.49 - 99.28)	97.29 (92.59 - 99.24)	97.55 (93.65 - 99.26)
Sensitivity (%)	96.03 (89.67 - 98.76)	95.59 (86.84 - 98.87)	96.10 (89.41 - 99.26)
Specificity (%)	98.70 (91.50 - 99.75)	98.12 (89.01 - 99.65)	98.31 (91.05 - 99.73)
PPV (%)	91.91 (70.87 - 99.24)	90.01 (64.22 - 98.86)	90.79 (67.78 - 99.12)

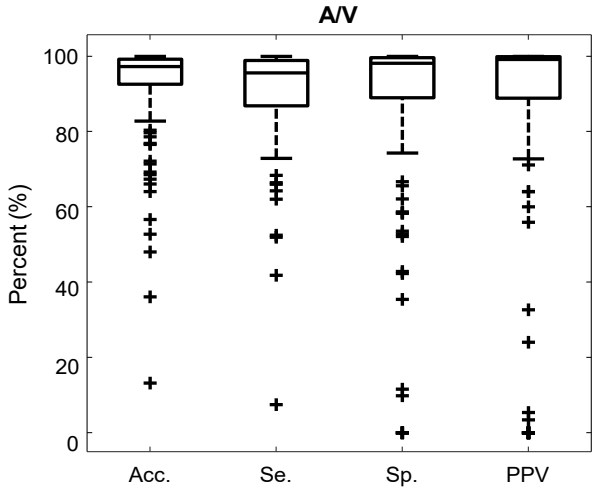

Figure 2. Boxplot of classification performance per patient for RR input Poincaré Images. Acc stands for accuracy, Se. for sensitivity and Sp. for specificity

This work intends to introduce a methodology to identify regions of interest of the ECG to localize A/V beats. Current beat classifiers focus on single beat classification, most attaining specially low performance on atrial beat detection [4,5] and thus, not suitable for the study of PAC implications. ECG segment classification could ease the selection of signal regions containing PACs or other types of A/V beats and serve to reduce false positives and identify possible false negatives. Differently, for manual beat annotation, it could reduce considerably the segments of the ECG for the clinician to analyse. As a future work other beat-windows could be explored. In addition, it could be explored how the implementation of this method as a prior classifier to with beat-to-beat classifiers could influence their performance.

5. Conclusion

In this paper an ECG segment classifier is introduced for the detection of segments containing A/V beats. The results obtained suggest this methodology could be used to reduce the ECG beat annotation workload to study PACs and other A/V implications. In addition, it could be used in combination with automatic beat classifiers to find misclassifications and obtain more reliable annotations.

Acknowledgments

This project is framed inside MY-ATRIA consortium. MY-ATRIA project has received funding from the European Union's Horizon 2020 research and innovation program under the Marie Skłodowska-Curie grant agreement No.766082.

References

[1] Chong Bh, Pong V, Lam Kf, Liu S, Zuo Ml, Lau Yf, Lau Cp, Tse Hf, Siu Cw. Frequent premature atrial complexes predict new occurence of atrial fibrillation and adverse cardiovascular events. Europace 2011;14:942–947.

[2] Huang BT, Huang FY, Peng Y, Liao YB, Chen F, Xia TL, Pu XB, Chen M. Relation of premature atrial complexes with stroke and death: Systematic review and meta-analysis. Clinical Cardiology 2017;40(11):962–969. ISSN 19328737.

[3] Larsen BS, Kumarathurai P, Falkenberg J, Nielsen OW, Sajadieh A. Excessive Atrial Ectopy and Short Atrial Runs Increase the Risk of Stroke beyond Incident Atrial Fibrillation. Journal of the American College of Cardiology 2015; 66(3):232–241. ISSN 15583597.

[4] Luz EJdS, Schwartz WR, Cámara-Chávez G, Menotti D. ECG-based heartbeat classification for arrhythmia detection: A survey. Computer Methods and Programs in Biomedicine 2016;127. ISSN 18727565.

[5] Llamedo M, Martinez JP. An automatic patient-adapted ECG heartbeat classifier allowing expert assistance. IEEE Transactions on Biomedical Engineering 2012;59(8):2312–2320. ISSN 00189294.

[6] Garcia-Isla G, Corino VD, Mainardi L. Poincaré Plot image and rhythm-specific atlas for atrial bigeminy and atrial fibrillation detection. IEEE Journal of Biomedical and Health Informatics 2020;25(4):1–1. ISSN 2168-2194.

[7] Goldberger AL, Amaral LAN. PhysioBank, PhysioToolkit, and PhysioNet. Circulation 2012;101(23):215–220. ISSN 0009-7322.

Address for correspondence:

Guadalupe García-Isla
Via Camillo Golgi 39, 20133 Milano, Italy
guadalupe.garcia@polimi.it